Comparison of Two Models on Simulating Electric Field in HVDC Cable Insulation

Yunpeng Zhan, George Chen and **Miao Hao**
University of Southampton
Southampton, SO17 1BJ, UK

Lu Pu, Xuefeng Zhao, Haofei Sun, Sen Wang, Anxiang Guo and **Jian Liu**
State Grid Shaanxi Electric Power Research Institute
Xi'an, 710100, China

ABSTRACT

Space charge accumulation in cable insulation is one of the major technical problems in the further development of HVDC cables. A conductivity model and a bipolar charge transport model are developed to respectively calculate the space charge and electric field distribution in polymeric insulation. In this paper, both models are employed to simulate the field distribution in a medium voltage polymeric cable. Comparisons are made between theoretical and simulation results. The limitations of the conductivity model which is widely used in HVDC cable design are presented, and the results of the bipolar charge transport model are more consistent with the experimental observations. Moreover, transient current in the cable is simulated to anticipate the field distribution within the insulation when subjected to a thermal transient. The results suggest that the thermal transient can affect the space charge and electric field distribution significantly. A field inversion can only take place with higher temperature and larger temperature gradient, and this can be maintained even with temperature decreasing.

Index Terms — **HVDC cable, bipolar charge transport model, thermal transient, field inversion**

1 INTRODUCTION

WITH the increasing demand of long distance power transmission and the rapid growth of renewable sources of electricity generation, HVDC cables have attracted more interest [1]. Moreover, it is believed to be the only solution for sea-crossing energy transfer [2]. Extruded insulation has been widely utilized for both HVAC and HVDC cable systems in the past decades [3]. The insulation material used in HVDC cable system requires special considerations, as the field distribution does not follow the same rules as for AC stress. In AC cables, the electric field E_{AC} depends on the permittivity ε of the dielectric, which changes little with temperature and field. On the contrary, the electric field E_{DC} in DC cables becomes conductivity σ dependent, which in turn depends on the temperature and E_{DC} [1]. Anticipating DC field distribution in polymeric insulation is more challenging when considering space charge phenomena. The space charge may build up in the bulk of insulation under various temperature and electric fields, and the presence of space charge can lead to the local field enhancement, which may accelerate material ageing or cause electrical failures [4].

In addition to improve the insulation material and minimize space charge effect, modelling and simulation is extremely useful to understand and predict material performance. Several calculations of the electric field and space charge distribution within the extruded cable insulation have been published, and such approaches are an importance reference for HVDC cable design [5, 6]. However, the limitations of such models have been recognized as the results are generally different from the experimental observations [7]. This may be due to the fact that the complicated conduction mechanisms such as charge injection are neglected. In contrast, a bipolar charge transport model, describes the details of charge generation mechanisms at the interface of electrode/dielectric and the charge transport processes (trapping, de-trapping and recombination) inside the bulk. It has been successfully applied in planar polymeric samples to study space charge and the results have achieved a good fit with experimental data [8]. However, only few attempts have been made to investigate the space charge dynamics in cable insulation [9]. Besides, the charge generation and transportation processes can be greatly affected by the temperature. Therefore, it is essential to consider thermal transient effects in modelling, in order to predict the field variation across the HVDC cable subjected to load cycles.

In this paper, both the conductivity model and the bipolar charge transport model are employed to simulate the field variation and charge distribution in a MV size XLPE cable. Comparisons are made between theoretical and simulation results. In addition, a changing current flow is applied in the core of cable to study the effect of thermal transients in both models.

Manuscript received on 16 October 2018, in final form 31 January 2019, accepted xx Month 20yy. Corresponding author: Y. Zhan.

2 BACKGROUND

From a macroscopic point of view, insulating materials allow a weak electrical conduction under DC field. This weak flow of charge within the insulation may not be uniform due to a local non-homogeneity of the material, thereby forming space charge. For a loaded cable, the presence of temperature gradient across the insulation may be accountable for the inhomogeneity, as the electrical conductivity of the insulating material strongly depends on the temperature. Investigations of space charge in the thermally pre-treated XLPE cable insulation with temperature gradients have been done by means of a modified PEA system, and the results showed the presence of temperature gradient could enhance the charge accumulation greatly, even might invert the electric field in cable insulation, as shown in Figures 1 and 2 [10, 11].

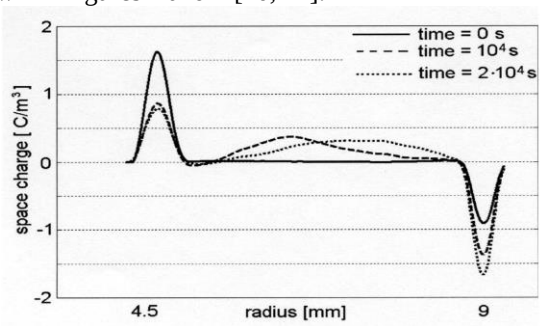

Figure 1. Space charge accumulation under a steady temperature gradient (65-45°C) in a MV size XLPE cable [10]. (Applied voltage 90 kV).

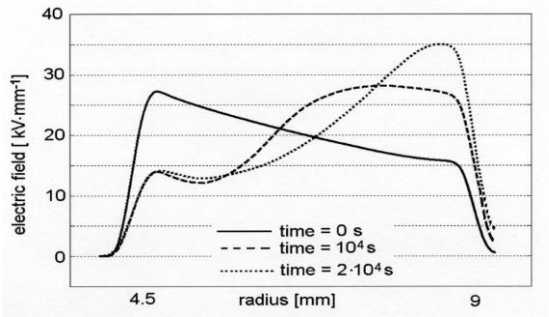

Figure 2. Electric field distribution across the insulation under a steady temperature gradient (ΔT=20 °C) in a MV size XLPE cable [10].

Based on the conductivity function, a macroscopic model was developed to predict the space charge and electric field distribution in loaded cable systems [6]. According to the current density continuity equation, when a divergence takes place between the incoming and outgoing charge, charge builds up in this region,

$$\nabla \cdot \vec{j} = -\frac{\partial \rho}{\partial t} \tag{1}$$

where j is the current density, ρ is the space charge density and t is the time. According to Gauss' Law and Ohm's Law,

$$\rho = \nabla \cdot \left(\varepsilon_0 \varepsilon_r \vec{E}\right) \tag{2}$$

$$\vec{j} = \sigma \vec{E} \tag{3}$$

By combining these three equations, the space charge density is given as:

$$\rho = -\frac{\varepsilon_0 \varepsilon_r}{\sigma}\frac{\partial \rho}{\partial t} + \vec{j} \cdot \nabla\left(\frac{\varepsilon_0 \varepsilon_r}{\sigma}\right) \tag{4}$$

Space charge ρ accumulates if the ratio between relative permittivity ε_r and conductivity σ were not uniform across the insulation, in the case of $j \neq 0$. The permittivity can be considered as a constant within the range of temperatures and DC fields, but the conductivity has to be considered as a function of both temperature and field. An expression of the conductivity with Arrhenius' Law has been widely used to describe the conductivity of the cable insulation [12],

$$\sigma(E,T) = A \cdot \exp\left(\frac{E_a}{k_B T}\right)\frac{\sinh(B|E|)}{|E|} \tag{5}$$

where E_a is the thermal activation energy; k_B is the Boltzmann's constant; constants A and B are determined by the characteristics of the insulation material. The parameters in the above equation could be obtained by fitting the conductivity function with the experimental results of conduction current measurements. Therefore, a time-varying conductivity gradient could be formed across the DC insulation due to the presence of temperature gradient, and the space charge and electric field distribution can be calculated straightforward by such model.

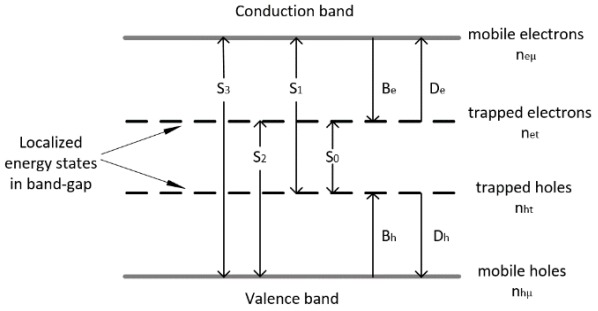

Figure 3. Schematic representation of the bipolar charge transport model. S_i, B_i and D_i are recombination, trapping and de-trapping coefficients respectively. n_i is the charge density. Indexes e and h refer to electrons and holes; μ and t refer to mobile and trapped charge carriers [8].

A bipolar charge transport model, which was firstly proposed by Alison and Hill in 1994 for simulation of charge profiles in degassed XLPE insulation [13], starts from the injection of positive and negative charge carriers at the interface of the insulation/electrodes when the applied electric field exceeds the threshold field. The injected electrons and holes move into the bulk of dielectrics towards the opposite electrodes under the influence of the electric field, forming the conduction current. Due to the localized energy states existing in the band-gap of the dielectrics, these "traps" may capture holes and electrons, forming trapped charge. Moreover, the trapped holes/electrons also have the possibility to escape from these "traps". Therefore, four species are considered in the model, mobile electrons/holes, trapped electrons/holes, as shown in Figure 3. In the bipolar charge transport model, three space and time dependent equations are presented to describe the charge behaviour in cylindrical geometry as following, neglecting diffusion,

Poisson's equation (in cylindrical coordinates):

$$\frac{\partial^2 V(r,t)}{\partial r^2} + \frac{1}{r}\frac{\partial V(r,t)}{\partial r} = -\frac{\rho(r,t)}{\varepsilon_0 \varepsilon_r} \tag{6}$$

Continuity equation:

$$\frac{\partial n_{a\mu,at}(r,t)}{\partial t} + \frac{1}{r}\frac{\partial (j_a \cdot r)}{\partial r} = s_{a\mu,at}(r,t) \quad (7)$$

Ohm's Law:

$$j_a(r,t) = \mu_a(r,t) n_{a\mu}(r,t) E(r,t) \quad (8)$$

where j_a is the conduction current density; n is the charge density; E is the electric field; ρ is the net charge density; ε_0 is the vacuum permittivity, ε_r is the relative dielectric permittivity, which is considered as a constant (2.3 for polyethylene). Here a refers to the type of charge, and the subscript μ or t refers respectively to mobile or trapped charge. s are the source terms which encompass the changes in local density by the processes other than transport (trapping, detrapping and recombination). For mobile electrons, $s_{e\mu}$ can be expressed as:

$$s_1 = \frac{\partial n_{e\mu}}{\partial t} = -S_1 n_{ht} n_{e\mu} - S_3 n_{h\mu} n_{e\mu} - B_e n_{e\mu}\left(1 - \frac{n_{et}}{n_{oet}}\right) + D_e n_{et} \quad (9)$$

The conduction is described by using a hopping type mobility between shallow traps as a function of field and temperature [9]. Additionally, the detrapping coefficients and the recombination coefficients are also functions of temperature and they have been described already in literature [9]. From the previous work done by Liu *et al* [14], a value of threshold electric field about 10 kV/mm has been identified for charge injection in polyethylene. In this study, when the applied field exceeds the critical value (10 kV/mm), the Schottky injection law is defined to be dominating and the linear field-dependent Ohmic conduction takes over under the low field [15]. It should be noted that the extraction barriers of charge carriers are not considered, and the extraction fluxes for holes at the cathode and for electrons at the anode follow the Equation (8).

3 COMPARISONS OF THE RESULTS

In this section, both models have been employed to simulate the space charge and electric field distribution in a medium-voltage size XLPE cable. The inner radius (r_i) of the cable is 4.5 mm, and the outer radius (r_o) is 9 mm, providing an insulation thickness of 4.5 mm. A positive voltage of 90 kV is applied at the inner electrode and a steady temperature gradient that derived from the thermal Ohm' Law has been applied across the insulation. The inner temperature is set to be 65°C and the outer temperature is 45°C. All the electrical and thermal conditions were set to be same as the experimental measurements [16], so the results of both models can be compared with the experimental observations.

3.1 SIMULATION RESULTS OF THE CONDUCTIVITY MODEL

The parameters used in the conductivity model are shown in Table 1, and they were obtained from fitting the conductivity function with the conduction current measurements on the thermally pre-treated XLPE specimens [10]. It should be noted that the activation energy adopted in this work is fairly high in comparison with the values usually found in the literature for XLPE [12]. However, in this work, the adopted activation energy does not characterize the XLPE insulation alone, but it includes the effect that the semi-conductive electrodes have on the conduction in the XLPE.

Table 1. Parameters used for the conductivity model

Parameter	Value	Unit
A	$1*10^{14}$	Am^{-2}
B	$2*10^{-7}$	$V^{-1}m$
E_a	1.48	eV

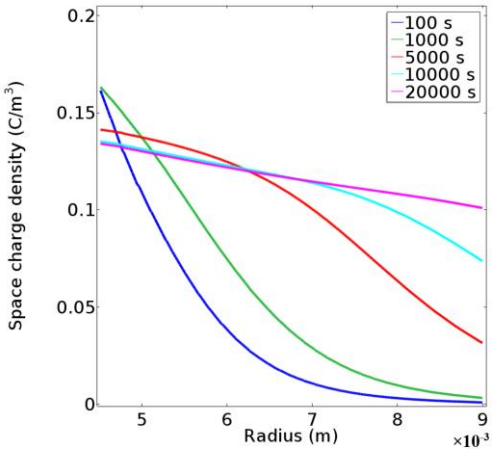

Figure 4. Simulated space charge profiles in the MV size cable insulation subjected to a steady temperature gradient (65-45°C).

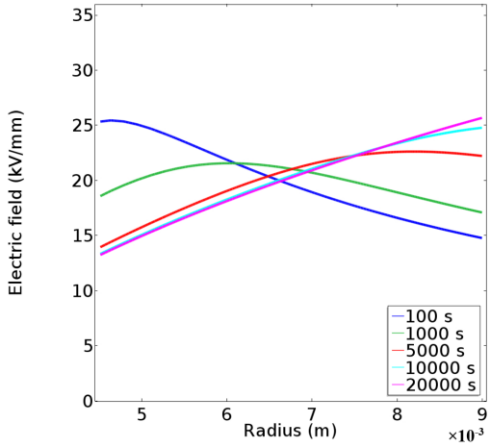

Figure 5. Calculated electric field distribution in the MV size cable insulation subjected to a steady temperature gradient (65-45°C).

The accumulation of charges is shown in Figure 4 due to the presence of temperature gradient. Only one-polarity space charge can be observed in the bulk, and the sign is same as the voltage on the inner electrode. At the beginning, very limited charges can be observed at the outer electrode, conversely, much more charges are accumulated at the inner insulation. With the time increasing, due to the strong temperature dependency of the conductivity, charge carriers will move fast in the inner part but shift slow in the outer part, namely a large amount of charge carriers accumulate inside the bulk. At t=20000 s, the average of the space charge density in the insulation bulk is about 0.12 C/m^3.

The calculated electric field distribution is shown in Figure 5. When the DC field is first applied, the electric field distribution is mainly decided by the permittivity of the insulation, and the insulation close to the conductor withstands the highest electric stress. Because of the presence of a steady temperature gradient (65-45°C), the conductivity at the inner side is extremely large while that of the outer area is relatively small. Therefore, the electric field near the conductor will decrease considerably, but

increase in the outer area. Under this 20°C temperature gradient, the field inversion phenomenon is predicted by this model so that the highest stress transfers from the inner to the outer insulation. It is believed that the field inversion limits the temperature rating of HVDC cables [17]. Therefore, it is very important to predict the field distribution at different operation stages, taking into account different environmental factors, due to the high dependence between conductivity and temperature.

3.2 SIMULATION RESULTS OF THE BIPOLAR CHARGE TRANSPORT MODEL

The parameters used in the bipolar charge transport model are given in Table 2, and these are mostly the ones that have been optimized from measurements achieved on space charge for a plane parallel LDPE [9].

Table 2. Parameters used for the simulations

Parameter		Value	Unit
Injection barrier heights	W_{ei} **for electrons**	1.27	eV
	W_{hi} **for holes**	1.16	eV
Trapping coefficients	B_e **for electrons**	0.1	s^{-1}
	B_h **for holes**	0.2	s^{-1}
Trap depths (for mobility)	w_{pe} **for electrons**	0.71	eV
	w_{ph} **for holes**	0.65	eV
Trap densities	n_{oet} **for electrons**	100	C/m^3
	n_{oht} **for holes**	100	C/m^3
Detrapping barrier heights	W_{tre} **for electrons**	0.96	eV
	W_{trh} **for holes**	0.99	eV

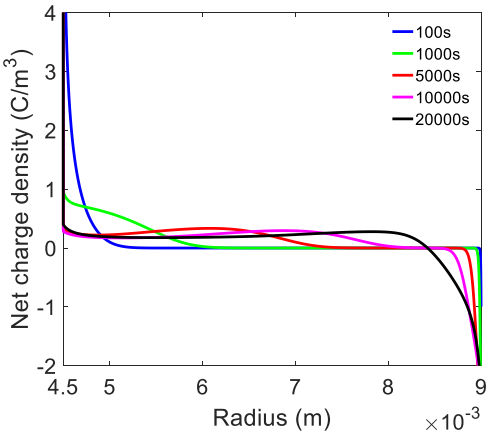

Figure 6. The simulated space charge density profiles in cylindrical geometry with a steady temperature gradient across the insulation.

When the DC vol0tage is applied, holes and electrons are injected from the anode and the cathode respectively, moving towards the opposite electrode under the influence of electric field, as shown in Figure 6. It is observed that a large amount of holes have penetrated into the volume with the time increasing, but the electrons seem to remain at the vicinity of the cathode and the movement of them is not obvious as holes. Until t=20000 s, the bulk has been charged adequately with holes and electrons. The presence of extensive homo-charges near the electrodes strongly decrease the electric field, especially at the anode, leading to an approximately non-injecting electrode shortly after the application of voltage, as presented in Figure 7.

The field variation within the insulation follows the movement of positive and negative charge carriers. With the time increasing, it can be observed that the maximal electric field location shifts from the anode to the cathode gradually. Namely the so-called stress inversion phenomenon, which has been widely reported in loaded HVDC cables, can be simulated by the bipolar charge transport model. At t=20000 s, the maximal electric field at the outer insulation has reached 34 kV/mm. It can be argued that the simulation results from the bipolar charge transport model, such as the movement and distribution of charge carriers, are more comparable with the experimental observations shown in Figures 1 and 2.

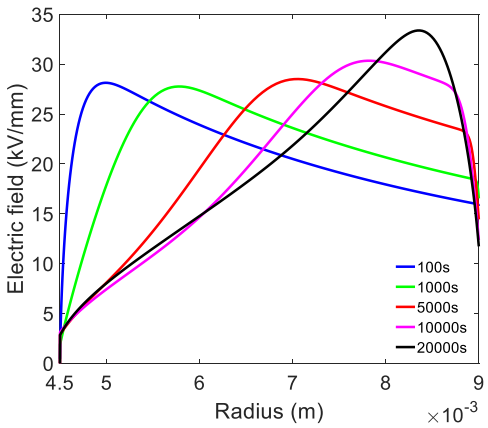

Figure 7. The electric field distributions in cylindrical geometry with a steady temperature gradient across the insulation.

3.3 COMPARISONS

It is assumed that the radial space charge distribution within the cable insulation is the same along the whole cable, independently on the axial and the angular position. Therefore, both the two models are resolved in 1-dimension, function of radius, and the simulated results from both models can present appropriate features on charge behavior and electric field distribution on the same cable insulation. The field inversion can be observed with both models under the steady temperature gradient. However, some differences still presents when compared with the experimental results.

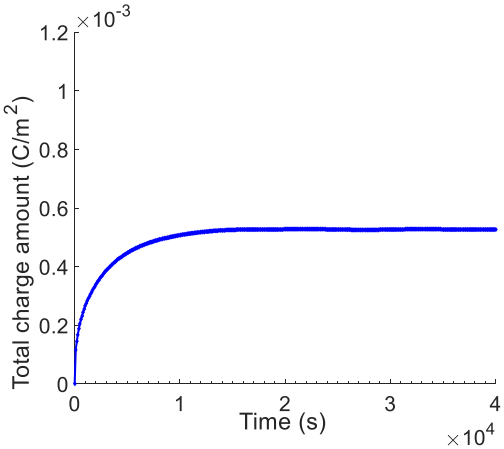

Figure 8. The total charge amount evolving with time calculated by the conductivity model.

When comparing the results of the conductivity model with the experimental data in Figures 1 and 2, at t=20000s, the electric field at the cathode was fairly underestimated; Moreover, the space charge distribution cannot correspond the experimental observations, as only one-polarity charge is considered in the conductivity model. Figure 8 shows the total

charge amount within the insulation for the conductivity model. It has to be announced that the accumulated charges are contributed from all types of charge carriers, including holes, electron and ions, as the parameter conductivity considers the overall contribution that each type of charge carriers has on the conduction process. The total charge amount within the bulk increased dramatically in the first 10000s, and then maintained at about 5.2×10^{-4} C/m^2 for the rest of time. The formation of the accumulated charges in the conductivity model is considered to be originated from the inhomogeneity of the current density across the insulation. At first, when the conductivity gradient along the radius of the insulation is steep, due to the presence of temperature gradient and the divergent field, charges would accumulate quickly. The variation of electric field could decrease the conductivity gradient and counterbalance the dissimilarity of the current density along the insulation. However, each kind of charge carriers behaves differently on the conduction process. The mobility, the possibility of being trapped and de-trapped and even recombination could be different from others, therefore, it might be not appropriate to consider the overall contribution of them. Besides, no information is provided about charge injection at the interface, but the charge accumulation at the interface affects the electric field distribution. Moreover, the equivalent insulation is considered to have a conductivity function of which the parameters do not depend on the position. However, at the interface of the electrode/insulation, the conductivity may differ from the one inside the bulk, due to the surface effect [18].

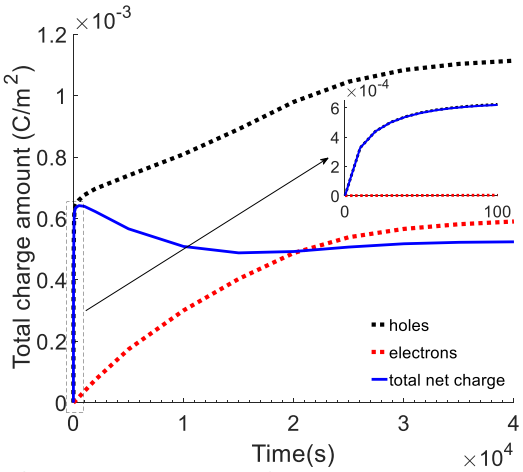

Figure 9. The total charge amount for positive and negative charge carriers evolving with time computed by the bipolar charge transport model.

The total charge amount of holes and electrons (including trapped and mobile) inside the bulk for the bipolar charge transport model are shown in Figure 9. Shortly after the application of DC voltage, much more holes are injected from the anode compared with electrons, and this large amount of positive homo-charges strongly decreases the field strength at the anode, which suppress the injection of holes. This is a consequence of higher temperature at the inner side and lower Schottky injection barrier for holes. Therefore, the total net charge amount inside the bulk increased very rapidly in the first 100s. Due to the injection of electrons and the interaction between holes and electrons, the total net charge amount decreased and maintained at about 5.1×10^{-4} C/m^2 since 15000s, which is approximate with the total charge amount calculated by the conductivity model at the stationary state. It is a very important evidence that can proof the conductivity function takes into account the overall contribution from all kinds of charge carriers on the conduction process. Note that the bipolar charge transport model does not consider the ionization process, which might be accountable for the difference. In spite of this, both the charge movement and the field variation seem to be more consistent when compared with the experimental data, as it gives very well descriptions on charge injection from the electrodes and charge transportation mechanisms inside the bulk. However, it is more complex when using the model in practical applications, as many parameters need to be taken into account carefully. The parameters that related to charge generation and transportation mechanisms cannot be obtained with a straightforward way by independent experiments. At present, the full parameterization is still demanding. Moreover, the treatment of physical processes like ionization and hetero-charge build-up is not considered, which also limits its performance.

4 THERMAL TRANSIENT

In loaded HVDC cable systems, the current flowing in the conductor varies with the transmission power, and the temperature gradient across the insulation varies at different operational stage. Due to the high temperature dependence, charge injection and transportation processes can be highly affected by thermal transient states. Therefore, it is essential to study the space charge dynamics and electric field variation under thermal transient. Heat transfer can be described as the movement of energy due to temperature dissimilarity. Base on the time dependent heat transfer equation shown as following, the temperature distribution across the insulation at each time step could be obtain,

$$\rho_d C_p \frac{\partial T}{\partial t} = \nabla \cdot (k \nabla T) + Q \tag{10}$$

where ρ_d is the material density; C_p is the heat capacity at constant pressure; k is the thermal conductivity; Q is the heat generated from the conductor, of the form:

$$Q = \frac{I^2 \rho_{al}}{A^2} \tag{11}$$

where A is the cross section area of the conductor; I is the DC current; ρ_{al} is the resistivity of the cable core. The boundary condition is set to be convective heat flux at the outer surface of insulator. It has been identified that when a current of 300 A is applied to the core of the MV size cable, a quasi-equilibrium (65-45°C) can be reached after 2 hours with a temperature gradient of ~20 °C. Similarly, a ~10 °C temperature gradient (40-30°C) across the insulation can be reached after 2 hours with a current of 200 A is applied into the core of cable. In the first case, the current flow in the conductor is set to be 200 A for the first 20000 s, then change into 300 A for the rest 20000 s. In this situation, the temperature gradient inside the bulk is raised and maintained at 40-30°C in the first period, and then raised and maintained at 65-45°C in the rest of time.

Under this thermal transient state, both the conductivity model and the bipolar charge transport model are employed to simulate the field variation and the space charge distribution.

The space charge distribution evolving with time calculated by the conductivty model is shown in Figure 10. As it presents, the charges accumulate very slow in the first 20000 s, and few charges can be observed at the outer electrode. After 20000 s, more charges are accumulated insider the bulk, and the final charge distribution is comparable with the one shown in Figure 4. The electric field variation across the insulation is presented in Figure 11. In the first 20000 s, when the temperature gradient is relatively small, the maximum electric field remains near the anode and slightly decreases, and the electric field at the cathode slightly increases. However, the field distribution inverses quickly after 20000 s, when the temperature gradient becomes larger.

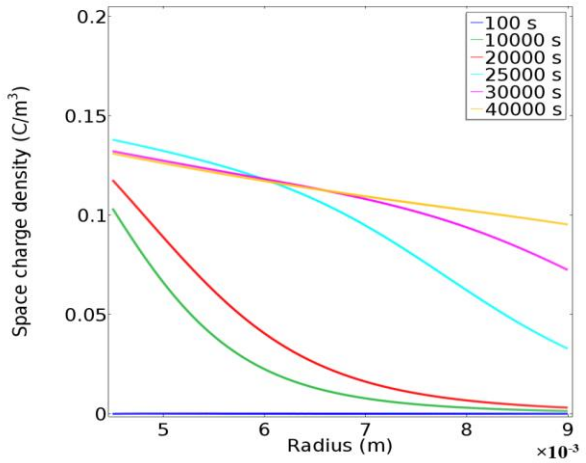

Figure 10. The space charge distribution across the insulation with a changing current (200 A-300 A) flowing in the core of cable, calculated by the conductivity model.

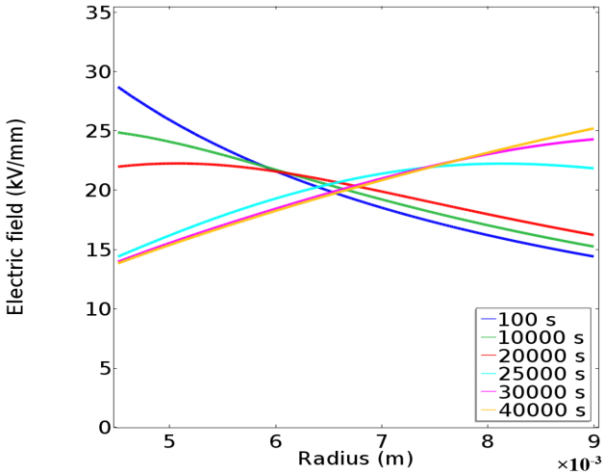

Figure 11. The electric distribution across the insulation with a changing current (200 A-300 A) flowing in the core of cable.

Figure 12 shows the space charge density profiles calculated by the bipolar charge transport model under this transient temperature distribution. Both the holes and electrons can be observed near the electrodes at the beginning but it seems that they do not penetrate into the volume. Until t=20000 s, both positive and negative charge carriers still remain near the electrodes. After 20000 s, the temperature across the insulation is increased significantly, so is the mobility for each type of charge carriers, therefore both holes and electrons can move into the bulk quickly. Compared with the results shown in Figure 6, the space charge distribution at the end is very similar. This is particularly surprising as the temperature distribution is very different in the first 20000 s, as if the initial low temperature distribution cannot affect the final charge distribution across the insulation.

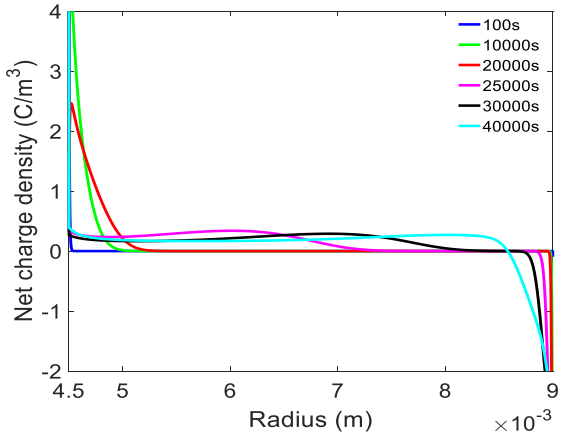

Figure 12. The simulated space charge density profiles with a changing current (200 A-300 A) flowing in the conductor, simulated by the bipolar charge transport model.

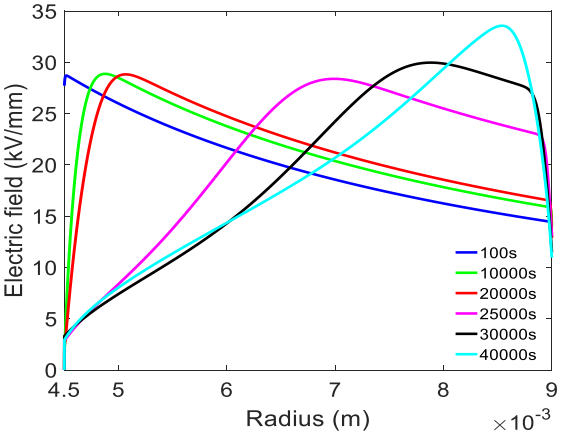

Figure 13. The simulated electric field distribution evolving with time with a changing current (200 A-300 A) flowing in the conductor.

The electric field variation across the insulation is shown in Figure 13. It can be observed that the maximal electric field location remains at the inner electrode in the first period (t<20000 s), and the variation is very limited. However, when the general temperature increases and the temperature gradient reaches 20 °C, the maximal electric field location shifts to the outer electrode gradually. The stress inversion phenomenon is not predicted when the general temperature is low and the temperature gradient is small. Only when it comes to the higher temperature and the larger temperature gradient, the stress inversion can take place. Additionally, the value of the maximal electric field at the end is almost same with that shown in Figure 7, but its location is closer to the cathode. This could be explained by the different thermal condition, which affects the injected charge amount and charge movement.

In another case, the current flow is set to be 300 A for the first 20000 s and then changed to 200 A for the rest of time. Therefore, the general temperature inside the volume is raised and maintained at 65-45°C in the first 20000 s, and then it is descended and maintained at 40-30°C in the rest of time.

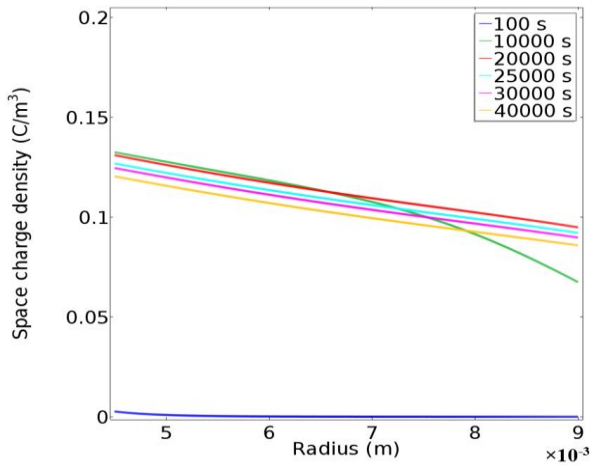

Figure 14. The space charge distribution calculated by the conductivity model with a changing current (300-200 A) flowing in the cable core.

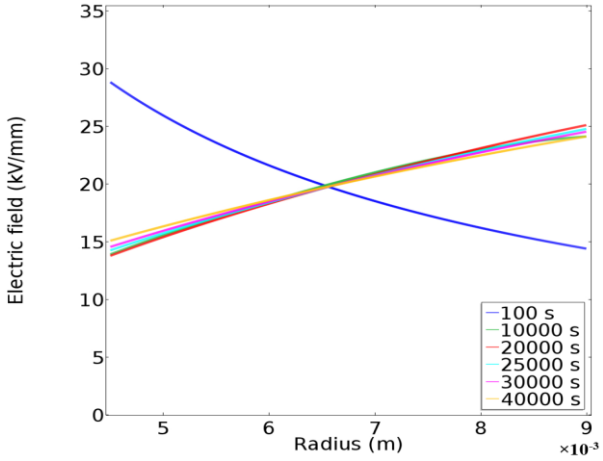

Figure 15. The electric field variation across the insulation with a changing current (300 A-200 A) flowing in the core of cable.

The space charge distribution evolving with time calculated by the conductivity model is shown in Figure 14. In the first stage (t<20000s), differently from the result shown in Figure 10, extensive charges are observed to accumulate inside the insulation bulk. Until t= 20000 s, the bulk is charged fully already. However, after t=20000 s, when the temperature distribution is decreased across the insulation, the overall accumulated charges decreased slightly. It is due to the magnitude of the conductivity gradient across the insulation decreases significantly with the temperature dropping, so is the magnitude of the current density gradient. The conductivity function becomes more field-dependent and less temperature-dependent at this lower temperature condition, therefore, the current density at the inner insulation decreases more quickly than the one at the outer under the reversed field, leading to a gentler current density gradient. According to the relationship (4), the lower the conductivity, it takes more time to establish a steady-state resistive field [19]. From t=20000 s to t=40000s, although the stationary state is not reached, the field strength at the inner electrode was raised by 1 kV/mm, and the one at the outer was descended by 1 kV/mm, as shown in Figure 15.

Figure 16 shows the space charge density profiles calculated by the bipolar charge transport model. During the first period (t<20000s), both holes and electrons penetrated quickly into the volume due to the high temperature distribution across the insulation. Interestingly, after the current flowing in the conductor is reduced to 200A, the distribution and the amount of charge carriers almost remain unchanged, and it seems to be frozen at the same position. The electric field distributions also behave in keeping with the space charge density profiles, as presented in Figure 17. The maximal electric field location shifted from the inner to the outer electrode in the first period, and then distribution remained consistent in the rest of time. It may be due the fact that the highly temperature-dependent mobility of both positive and negative charge carriers. The movement of charge carriers become extremely slow under this relatively low temperature condition. Moreover, very few charge carriers are injected from the electrodes due to the low electric field at the anode and the low temperature at the cathode after t=20000 s.

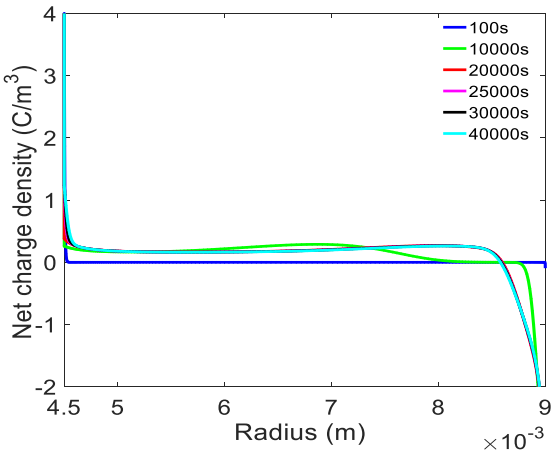

Figure 16. The simulated space charge density profiles with a changing current (300 A-200 A) flowing in the conductor, calculated by the bipolar charge transport model.

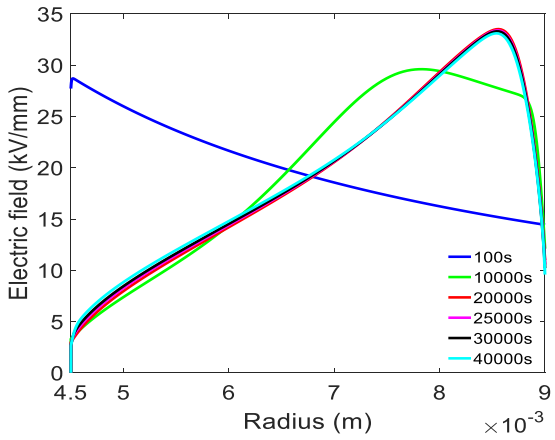

Figure 17. The electric field distribution with a changing current (300 A-200 A) flowing in the conductor.

From the results of both models, the predicted field inversion behaves similarly when the cable is subjected to a changing current. However, the differences, such as the deviation of electric field when the cable is subjected to a decreasing current, still presents between the two models. It must be emphasized that the space charge calculated by the conductivity model is independent of any space charge generation mechanisms. These delocalized charges accumulates at the inhomogeneities of conductivity. In contrast, the injection from the electrodes is the only source of space charge formation in the bipolar charge

transport model, and the charges may be localized and stored at certain trapping centres.

5 CONCLUSIONS

Both the macroscopic model and the bipolar charge transport model were employed to simulate the space charge and electric field distribution in a cable insulation. The following conclusions can be drawn.

With the presence of a steady temperature gradient, the well-known field inversion has been observed by both models. Compared with the experimental observations in a same size cable under the same electrical and thermal condition, the results of the bipolar charge transport model were more consistent, even with parameters that are not optimized for a XLPE material. The well descriptions on the charge injection at the interface and the complicated transportation processes were considered as the main reasons for the better performance of the bipolar charge transport model.

The cable was also subjected to a changing current to investigate the space charge and field variations under the transient temperature distribution. The results from both models show similar field variation. The field inversion can only take place with a high load current, while it is still present at a lower load current. The next step will be the space charge measurements in cable insulation under the thermal transient, and the ionization process will also be considered in further modelling.

ACKNOWLEDGMENT

The authors are grateful for the financial support from the technology project of State Grid Shaanxi Electric Power Company [5226KY16001G] and [2018GY-001].

REFERENCES

[1] G. Mazzanti and M. Marzinotto, *Extruded Cables for High-voltage Direct-current Transmission: Advances in Research and Development*, Power Engineering Series, Wiley-IEEE Press, 2013.

[2] H. Ghorbani, M. Jeroense, C.-O. Olsson, and M. Saltzer, "HVDC cable systems—highlighting extruded technology," IEEE Trans. Power Deliv., vol. 29, no. 1, pp. 414–421, 2014.

[3] G. Chen, M. Hao, Z. Xu, A. Vaughan, Cao, Junzheng, and H. Wang, "Review of High Voltage Direct Current Cables," 10 Csee J. Power Energy Syst., vol. 1, no. 2, pp. 9–21, 2015.

[4] M. Fu, L. A. Dissado, G. Chen, and J. C. Fothergill, "Space charge formation and its modified electric field under applied voltage reversal and temperature gradient in XLPE cable," IEEE Trans. Dielectr. Electr. Insul., vol. 15, no. 3, 2008.

[5] E. Ildstad, F. Mauseth, and G. Balog, "Space charge and electric field distribution in current loaded polyethylene insulated HVDC cables," *Int. Symp. HV Eng*, 2003, p. 366.

[6] P. H. F. Morshuis, R. Bodega, D. Fabiani, G. C. Montanari, L. A. Dissado, and J. J. Smit, "Calculation and Measurement of Space Charge in MV-size Extruded Cables Systems under Load Conditions," *IEEE Int. Conf. Solid Dielectrics (ICSD)*, 2007, pp. 502–505.

[7] T. T. N. Vu, G. Teyssedre, B. Vissouvanadin, S. Le Roy, C. Laurent, M. Mammeri, I. Denizet, "Field distribution in polymeric MV-HVDC model cable under temperature gradient: simulation and space charge measurements," Eur. J. Electr. Engg., vol. 17, pp. 307–325, 2014.

[8] S. Le Roy, G. Teyssedre, C. Laurent, G. C. Montanari, and F. Palmieri, "Description of charge transport in polyethylene using a fluid model with a constant mobility: fitting model and experiments," J. Phys. D. Appl. Phys., vol. 39, no. 7, p. 1427, 2006.

[9] S. Le Roy, G. Teyssedre, and C. Laurent, "Modelling space charge in a cable geometry," IEEE Trans. Dielectr. Electr. Insul., vol. 23, no. 4, pp. 2361–2367, 2016.

[10] R. Bodega, "Space charge accumulation in polymeric high voltage DC cable systems", PhD dissertation, Delft University of Technology, 2006.

[11] W. Choo, G. Chen, and S. G. Swingler, "Electric field in polymeric cable due to space charge accumulation under DC and temperature gradient," IEEE Trans. Dielectr. Electr. Insul., vol. 18, no. 2, 2011.

[12] S. Boggs, D. H. Damon, J. Hjerrild, J. T. Holboll, and M. Henriksen, "Effect of insulation properties on the field grading of solid dielectric DC cable," IEEE Trans. power Del., vol. 16, no. 4, pp. 456–461, 2001.

[13] J. M. Alison and R. M. Hill, "A model for bipolar charge transport, trapping and recombination in degassed crosslinked polyethene," J. Phys. D: Appl. Phys., vol. 27, pp. 1291–1299, 1994.

[14] N. Liu, C. Zhou, G. Chen, and L. Zhong, "Determination of threshold electric field for charge injection in polymeric materials," Appl. Phys. Lett., vol. 106, no. 19, p. 192901, 2015.

[15] Y. Zhan, G. Chen, and M. Hao, "Space charge modelling in HVDC extruded cable insulation," IEEE Trans. Dielectr. Electr. Insul., 2018.

[16] D. Fabiani, G. Montanari, C. Laurent, G. Teyssedre, P.H.F. Morshuis, R. Bodega, L.A. Dissado, "HVDC cable design and space charge accumulation. part 3: effect of temperature gradient," IEEE Electr. Insul. Mag., vol. 24, no. 2, pp. 5–14, 2008.

[17] Z. Y. Huang, J. A. Pilgrim, P. L. Lewin, and S. G. Swingler, "Real-time electric field estimation for HVDC cable dielectrics," *IEEE Electr. Insul. Conf. (EIC)*, 2015, pp. 1–4.

[18] S. Boggs, "A rational consideration of space charge," IEEE Electr. Insul. Mag., vol. 20, no. 4, pp. 22–27, 2004.

[19] C.-O. Olsson and M. Jeroense, "Evolution of the distributions of electric field and of space charge in an extruded HVDC cable," *8th Int. Conf. Insulated Power Cables (Jicable)*, 2011, vol. 2.

Yunpeng Zhan was born in in China in 1994. He received his B.Eng. degree (2016) in electronic science from Xiamen University, China. Since 2016, he has been a Ph.D student in University of Southampton, UK. His main research interests are space charge and insulation materials for HVDC cables.

George Chen (SM'11) was born in China in 1961. He received his B.Eng (1983) and M.Sc (1986) degrees in electrical engineering from Xi'an Jiaotong University, China. After he obtained the Ph.D. degree (1990) from the University of Strathclyde, UK, on the permanent changes in the electrical properties of irradiated low-density polyethylene; he joined the University of Southampton as a postdoctoral research fellow and subsequently became a senior research fellow. He is now a professor of high voltage engineering at the University of Southampton and a visiting professor of Xi'an Jiaotong University. He has developed a wide range of interests in high voltage engineering and electrical properties of materials and published over 300 papers.

Miao Hao was born in China in 1987. He received his B.Eng. degree (2009) from Xi'an Jiaotong University, China. After he obtained his M.Sc. degree (2011) and Ph.D. degree (2015) from University of Southampton. He is now a postdoctoral research fellow in the University of Southampton. His main research interests include space charge and ageing mechanism in dielectrics for HVDC applications.